Functional switching of GABAergic synapses by ryanodine receptor activation

Miao-Kun Sun*, Thomas J. Nelson, and Daniel L. Alkon

Laboratory of Adaptive Systems, National Institute of Neurological Disorders and Stroke, National Institutes of Health, Bethesda, MD 20892

Communicated by Bernhard Witkop, National Institutes of Health, Bethesda, MD, August 18, 2000 (received for review May 26, 2000)

The role of the ryanodine receptor (RyR) in modifiability of synapses made by the basket interneurons onto the hippocampal CA1 pyramidal cells was examined in rats. Associating single-cell RyR activation with postsynaptic depolarization increased intracellular free Ca^{2+} concentrations and reversed the basket interneuron–CA1 inhibitory postsynaptic potential into an excitatory postsynaptic potential. This synaptic transformation was accompanied by a shift of the reversal potential from that of chloride toward that of bicarbonate. This inhibitory postsynaptic potential–excitatory postsynaptic potential transformation was prevented by blocking RyR or carbonic anhydrase. Associated postsynaptic depolarization and RyR activation, therefore, changes GABAergic synapses from excitation filters to amplifier and, thereby, shapes information flow through the hippocampal network.

Memories are thought to be a result of lasting synaptic modifications in the brain structures related to information processing (1–3). Ca^{2+} signaling (4), controlled by the endoplasmic reticulum (ER) and the plasma membrane, is a critical factor that induces changes in synaptic plasticity (5, 6). Not only might neural activity control the amount of Ca^{2+} stored in the ER, but Ca^{2+} also can be released as a signal messenger to modify synaptic function, kinase activity, and protein synthesis (6, 7). Training rats in a spatial water-maze task has been found to increase ryanodine receptor (RyR_2) expression in the hippocampus (6). Elevated intracellular Ca^{2+} levels can spread through cells as global waves or be highly localized within spatially distinct compartments such as the terminals or dendritic spines (8, 9). Functional operation of neural synapses might be altered over long-lasting time domains by intracellular Ca^{2+} release, resulting in reshaping information processing in neural structures such as the hippocampus.

Here, we examined the effects of associating RyR activation with postsynaptic depolarization on GABAergic synaptic transmission in the hippocampal CA1 area. The CA1 pyramidal cells are innervated by GABAergic interneurons and receive glutamatergic inputs from CA3. Associated postsynaptic depolarization and activation of RyR receptors of CA1 cells produced a lasting reduction and reversal of the GABAergic inhibitory postsynaptic potential (IPSP) responses, converting excitation filters to amplifiers. The resulting synaptic plasticity is likely to redirect signal processing through the hippocampal network and may play an important role in hippocampus-dependent learning and memory.

Methods

Brain Slices and Electrophysiology. Male Sprague–Dawley rats (130–180 g) were anesthetized with halothane and decapitated, and the brains were removed and cooled rapidly in a modified artificial cerebrospinal fluid solution (aCSF; ≈4°C), bubbled continuously with 95% O_2 and 5% CO_2 (10, 11). Hippocampi were sliced (400 μM), with either a Vibratome or a McIllwain Tissue Chopper (Westbury, NY), placed in oxygenated aCSF (124 mM NaCl/3 mM KCl/1.3 mM $MgSO_4$/2.4 mM $CaCl_2$/26 mM $NaHCO_3$/1.25 mM NaH_2PO_4/10 mM glucose), and subfused (2 ml/min) with the oxygenated aCSF in a recording chamber (Medical Systems, Greenvale, NY) and allowed to equilibrate for a minimum of 1 h at 30–31°C. The cells were recorded by using either whole-cell patch or intracellular techniques. For whole-cell patch clamp, the slices were transferred and submerged in oxygenated CSF solution and inhibitory postsynaptic currents (IPSCs) were recorded with fire-polished [Narishige microforge (Tokyo), immediately before use] patch electrode (3–5 MΩ when filled with internal solution). The electrode solution contained 135 mM potassium gluconate, 5 mM NaCl, 2 mM $MgCl_2$, 10 mM Hepes, 2 mM Mg-ATP, and 0.3 mM Na-GTP (pH 7.25 with KOH). EGTA (1 mM) or Fura-2 (0.5 mM; Molecular Probes) and/or ruthenium red (RR; 20 μM) was added to the internal solution when indicated. Cells were visualized by infrared differential interference contrast microscopy (12) through a ×40 water-immersion objective. Input resistance in whole-cell mode was typically 100–200 MΩ. Changes in intracellular free Ca^{2+} concentration ($[Ca^{2+}]_i$) were measured with a cooled charge-coupled device camera. The recorded neuron was exposed to UV light only during the measurement of $[Ca^{2+}]_i$ to avoid photic damage of neurons. The correction for background fluorescence was performed by subtraction of the background levels, obtained by taking the value away from the recorded area. Fluorescence ratios (340:380 nM) were converted to intracellular Ca^{2+} concentrations by using the equation of Grynkiewicz *et al.* (13) with apparent dissociation constant, $K_d = 0.224$ μM, with R_{min} and R_{max} determined when $[Ca^{2+}]_i$ of the cells equilibrates with "calcium-free" (0 mM Ca^{2+}/10 mM EGTA) or high Ca^{2+} (10 mM Ca^{2+} in Hepes), respectively. For intracellular recordings, the CA1 pyramidal cells were recorded with sharp electrodes (tip resistance: 60–120 MΩ). Labeling the recorded cells reveals recording of the CA1 pyramidal cells (14). A major advantage of the intracellular microelectrode recording configuration over whole-cell clamp is the avoidance of internal perfusion of test agents into the cells and the running down of γ-aminobutyric acid (GABA)-evoked currents in the whole-cell patch configuration. A period of control without the immediate influence of test agents thus is possible and crucial for comparisons.

Bipolar stimulating electrodes (Teflon-insulated PtIr wire, 25 μm in diameter) were placed in stratum pyramidale, within 200 μm from the recording electrode, for stimulation of interneurons (50 μA, 50 μA) and in stratum radiatum to stimulate the Schaffer collateral pathway (SCH) in some cases. Studies were performed on CA1 neurons with stable resting membrane potentials more

Abbreviations: BAS, basket interneurons; BIC, bicuculline; cADP-ribose, cyclic ADP-ribose; $[Ca^{2+}]_i$, intracellular free Ca^{2+} concentration; EPSP, excitatory postsynaptic potential; GABA, γ-aminobutyric acid; IPSC, inhibitory postsynaptic current; IPSP, inhibitory postsynaptic potential; NEMM, *N*-ethylmaleimide; RR, ruthenium red; RyR, ryanodine receptor; SCH, Schaffer collateral pathway.

*To whom reprint requests should be addressed at: Laboratory of Adaptive Systems, National Institute of Neurological Disorders and Stroke/National Institutes of Health, Building 36, Room 4A24, 36 Convent Drive, Bethesda, MD 20892. E-mail: mksun@codon.nih.gov.

The publication costs of this article were defrayed in part by page charge payment. This article must therefore be hereby marked "*advertisement*" in accordance with 18 U.S.C. §1734 solely to indicate this fact.

Article published online before print: *Proc. Natl. Acad. Sci. USA*, 10.1073/pnas.210396697. Article and publication date are at www.pnas.org/cgi/doi/10.1073/pnas.210396697

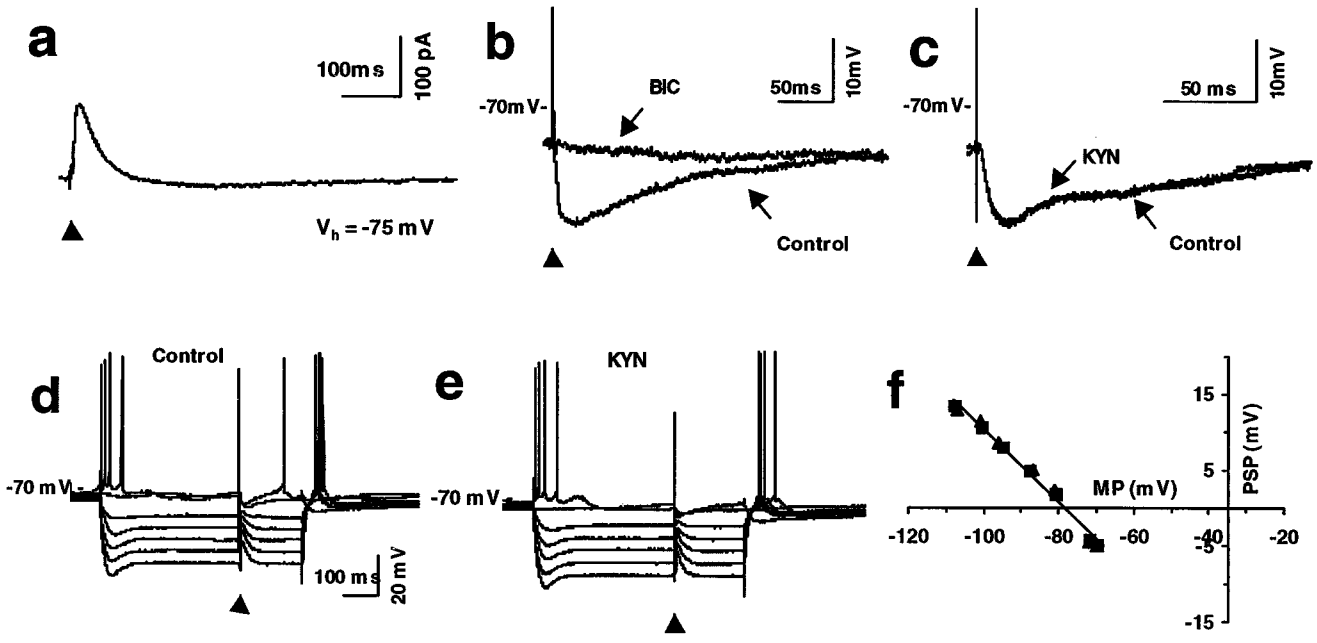

Fig. 1. Transformation of GABAergic BAS-CA1 synapses by RyR activation. (*a*) Stimulation of local GABAergic neurons elicited a monophasic IPSC recorded in a hippocampal CA1 pyramidal cell under whole-cell patch voltage clamp. BIC (1 μM, 30 min) eliminates (*b*) whereas kynurenate (KYN; 500 μM, 20 min) does not alter (*c*) the evoked IPSPs. (*d*—*f*) The relationship between the evoked BAS-CA1 PSP at different membrane potentials can be described with a straight line, determined by the least-sum squares criterion, and is not altered by kynurenate.

negative than −70 mV. Test stimuli were applied at a frequency of 1 per min (0.017 Hz). Signals were amplified with an AxoClamp-2B amplifier, digitized, and stored by using DIGIDATA 1200 with the P-CLAMP data collection and analysis software (Axon Instruments, Foster City, CA). Experiments in which >20% variations in the evoked IPSP or excitatory postsynaptic potential (EPSP) magnitudes during 10-min control periods occurred were discarded. Percent baseline PSP at each minute was calculated by dividing its value by baseline PSP and then multiplying the result by 100. The average IPSP value over a 10-min period before treatments in each cell thus was defined as 100% baseline PSP. A negative sign was added to indicate its inhibitory nature so that −100% indicates the average baseline IPSP and a positive value indicates an excitatory response. Differences were considered significant at $P < 0.05$.

Drugs and Chemicals. Agents were either injected into the recorded cells through the recording electrodes: cyclic adenosine diphosphate-ribose (cADP-ribose; 20 μM in internal solution; intracellular: −1.0 nA, 500 ms, 50% on cycles through 2-mM solution, 15 min), *N*-ethylmaleimide (NEMM; −1.0 nA, 500 ms, 50% on cycles through 200 mM solution, 15 min); RR (20 μM in internal solution; intracellular: +0.5 nA, 500 ms, 50% on cycles through 2 mM solution, 10 min); or through perfusion medium: kynurenic acid (500 μM; 20 min; refs. 10 and 15), bicuculline methiodide (BIC; 10 μM, 30 min). Unless otherwise specified, chemicals were obtained from Sigma.

Results

GABAergic interneurons in the hippocampus exert powerful control over hippocampal networks (16–20). Single-pulse stimuli to stratum pyramidale elicited IPSCs (peak response: 124 ± 8.5 pA, $n = 5$, whole-cell voltage clamp at −75 mV) or IPSPs, recorded intracellularly, in the CA1 pyramidal neurons at their resting membrane potential (Fig. 1 *a* and *b*). A gradual running-down of IPSCs was observed because of cell dialysis/washing out of intracellular components, whereas the IPSPs recorded intracellularly were stable for hours and thus were used for examining long-term GABAergic responses. The IPSP (−8.5 ± 0.2 mV, $n = 20$, $P < 0.05$) was largely or completely abolished (by 95.3 ± 3.3%, $n = 10$, $P < 0.05$, paired *t* test) by BIC, a GABA type A receptor antagonist (1 μM, 30 min). The sensitivity to BIC indicates that the evoked IPSP is mediated largely, if not exclusively, by activation of the basket interneuron (BAS)-CA1 pathway and involves GABA type A receptors.

Kynurenate, a wide-spectrum competitive antagonist for glutamate receptors (15), was used to reveal whether the stimulating current might spread to activate the SCH. Kynurenate blocks both NMDA and non-NMDA ionotropic subtypes, receptors for the most dominant excitatory inputs to the CA1 pyramidal neurons. At 500 μM (20 min; ref. 10), it effectively eliminated SCH-CA1 EPSPs (by >90%; not shown) but did not increase BAS-CA1 IPSP magnitudes (Fig. 1*c*). In the presence of kynurenate (20 min), the BAS-CA1 IPSP (−8.0 ± 0.3 mV, $n = 9$, $P < 0.05$) did not differ ($P > 0.05$, paired *t* test) from that before kynurenate application (−7.9 ± 0.3 mV, $n = 9$, $P < 0.05$). The BAS-CA1 IPSP reversed at a single-membrane potential (Fig. 1 *d–f*; −79.6 ± 0.4 mV, $n = 77$), revealing no obvious minor component that exhibits a different reversal potential. In all cases, the IPSP-membrane potential relations could be described with a straight line and were not affected by blocking the ionotropic glutamate receptors ($n = 9$; Fig. 1*f*).

CA1 pyramidal cells in the hippocampus, a region intensely studied for its importance in explicit memory, are characterized with greater abundance of the RyRs than the inositol trisphosphate receptors in their spines (21). The RyR agonist, cADP ribose (22), an endogenous metabolite of nicotinamide-adenine dinucleotide, was used to activate the RyRs (22). In the presence of extracellular 1 μM tetrodotoxin to block the generation of action potentials, cADP-ribose (20 mM internal solution) increased $[Ca^{2+}]_i$ (by 172 ± 11 nM on average, $n = 4$, $P < 0.05$; Fig. 2*a*) and depolarization-evoked increases in $[Ca^{2+}]_i$ (peak responses by 98.7 ± 8.2% on average, $n = 4$, $P < 0.05$; Fig. 2*a*). The cADP-ribose-induced increases in baseline $[Ca^{2+}]_i$ and

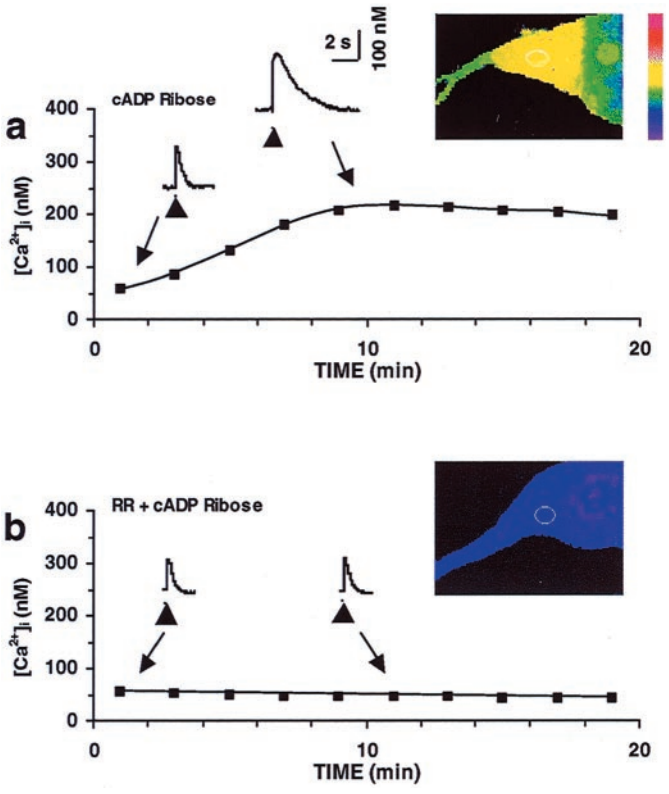

Fig. 2. Effects of cADP-ribose on $[Ca^{2+}]_i$ and depolarizing-induced $[Ca^{2+}]_i$ increases and sensitivity to RR. Under whole-cell voltage clamp, cADP-ribose increased $[Ca^{2+}]_i$ and the depolarizing-induced $[Ca^{2+}]_i$ increase (*Insets*) (*a*). The presence of RR in the internal solution eliminated cADP-ribose's effects on $[Ca^{2+}]_i$ and the enhancement of the depolarizing-induced $[Ca^{2+}]_i$ increase (*Insets*) (*b*). The zeros on the abscissas indicate the beginning of whole-cell patch formation. Depolarizing pulse was from −75 to −20 mV for 100 ms in duration. *Insets* (*Right*) Pseudocolor images of neurons about 10 min after the recording. Measurements of the ratiometric data were made in the somata near primary dendrites (white ovals; calibration bar = 50–500 nM).

depolarization-evoked $[Ca^{2+}]_i$ increase both were eliminated by RR (Fig. 2*b*; 20 μM internal solution), a membrane impermeant molecule that inhibits the RyRs with IC_{50} in the nanomolar range without affecting inositol trisphosphate receptor-mediated Ca^{2+} release (23), in four cells tested ($P > 0.05$ for the changes in $[Ca^{2+}]_i$ and depolarization-evoked changes). Intracellular injection of cADP-ribose (see *Methods*) into CA1 pyramidal cells produced a lasting (>1 h), significant reduction in magnitude (by 76.8 ± 7.8% 30 min after cADP-ribose, $n = 9$, $P < 0.05$) of the BAS-CA1 IPSP (Fig. 3*a*) without changing membrane input resistance. NEMM, a sulfhydryl reagent (23), also was used to activate the RyRs (22), yielding qualitatively and quantitatively similar results. The cADP-ribose- or NEMM-induced reduction in BAS-CA1 IPSP does not appear to result from a simple blockade of the involved receptor–channel complex. Rather, injection of each agent caused a shift (Fig. 3*c*) of the relationship between the BAS-CA1 PSP and membrane potential to the right and of the reversal membrane potential to a more positive potential (to −68.9 ± 2.2 mV about 30 min after cADP-ribose from −79.7 ± 2.0 mV about 5 min before cADP-ribose). The effects were prevented ($n = 7$) by RR (Fig. 3*d*). RR produced a period of enhanced magnitude of BAS-CA1 IPSPs (Fig. 3 *d* and *e*; by 20.5 ± 2.0%, $n = 15$, $P < 0.05$). The enhancement was not simply an increase in postsynaptic response for a given membrane potential. The relationship between BAS-CA1 IPSPs and membrane potential was shifted to the left (Fig. 3*f*). RR, thus, induced a significant change in the reversal potential to a more negative potential (to −87.7 ± 2.2 mV 30 min after, from −79.2 ± 2.0 mV 5 min before RR injection, $n = 15$, $P < 0.05$, paired *t* test). The observation that RR neither reduced synaptic responses nor affected postsynaptic membrane properties suggests that no significant amount got through the membrane to block voltage-sensitive Ca^{2+} channels and transmitter release, effects that otherwise would be observed.

Coapplication of cADP-ribose or NEMM with postsynaptic depolarization (to load Ca^{2+}) during the injection period reversed the BAS-CA1 IPSP to an excitatory response (Fig. 3*b*). The transformation thus requires a temporal association of RyR-mediated Ca^{2+} release with Ca^{2+} influx. The synaptic transformation did not occur suddenly but, rather, as an extension of an initial gradual reduction in the BAS-CA1 IPSPs, lasting for more than 1 h (Fig. 3*g*). The reversal potential of the BAS-CA1 PSPs 30 min after cADP-ribose depolarization was −65.3 mV (±2.4 mV), significantly differing ($n = 8$, $P < 0.05$, paired *t* test) from its control value (−78.7 ± 1.9 mV). RR application was effective in blocking the cADP-ribose depolarization- or NEMM depolarization-induced synaptic transformation. After RR injection, coapplication of cADP-ribose ($n = 8$) or NEMM ($n = 7$) with postsynaptic depolarization did not transform the synaptic responses. For instance, the BAS-CA1 IPSPs after RR-cADP-ribose depolarization were −118.9% (±2.6%, $n = 8$, $P < 0.05$), not significantly different ($n = 8$, $P > 0.05$) from −117.2% (±2.2% before cADP-ribose depolarization; $n = 8$, $P < 0.05$, paired *t* test). The effectiveness of RR indicates that the synaptic transformation depends on postsynaptic depolarization and associated RyR activation. The effects, however, were sensitive to carbonic anhydrase inhibition. In the presence of acetazolamide (1 μM, 30 min), a carbonic anhydrase inhibitor, cADP-ribose depolarization caused no obvious alterations in the BAS-CA1 IPSPs ($n = 7$; Fig. 3*h*).

Long-term synaptic transformation (11, 14) alters GABAergic synaptic sign as well as the amplitudes of the glutamatergic inputs, thereby providing a mechanism to selectively activate a subset of pyramidal neurons and block others. Such selective activation also may contribute to long-term synaptic potentiation. Activation of BAS produced fast IPSPs and reduces excitability and probability of action potential generation of the CA1 pyramidal cells (Fig. 4 *a* and *b*). SCH stimulation at intensities above (30%) threshold elicited action potentials (100% of 10 trials; Fig. 4*a*). BAS stimulation produced an effective signal-filtering period of 50–100 ms (up to 200 ms in some cases), during which no action potential (0% of 10 trials) was evoked by SCH stimulation at the same intensities (Fig. 4*b*; $n = 10$, $P < 0.05$). Action potentials were elicited reliably (Fig. 4*f*; 100% of 10 trials each cell; $n = 10$, $P < 0.05$) after cADP-ribose postsynaptic depolarization-induced transformation (Fig. 4*e*) by single-pulse costimulation of SCH (at below threshold) intensities and BAS. Before the cADP-ribose depolarization, the same intensities of costimulation did not evoke action potentials (Fig. 4 *c* and *d*; 0% of 10 trials each; $n = 10$). cADP-ribose postsynaptic depolarization also induced a brief period of reduction in afterhyperpolarization, which gradually recovered to its control values (Fig. 4*f*). Weak excitatory signals thus are amplified in those cells that receive transformed IPSPs, while allowing only very strong excitatory signals to successfully pass through those cells under normal BAS inhibition (Fig. 4*g*). Thus, opposite GABAergic effects in subsets of neurons could act as either filters or amplifiers.

Discussion

Controlled Ca^{2+} release from intracellular stores within a neuron represents an important mechanism for amplifying Ca^{2+} signals received from outside the neuron. Such intracellular release is also important for the generation of stimulus-specific

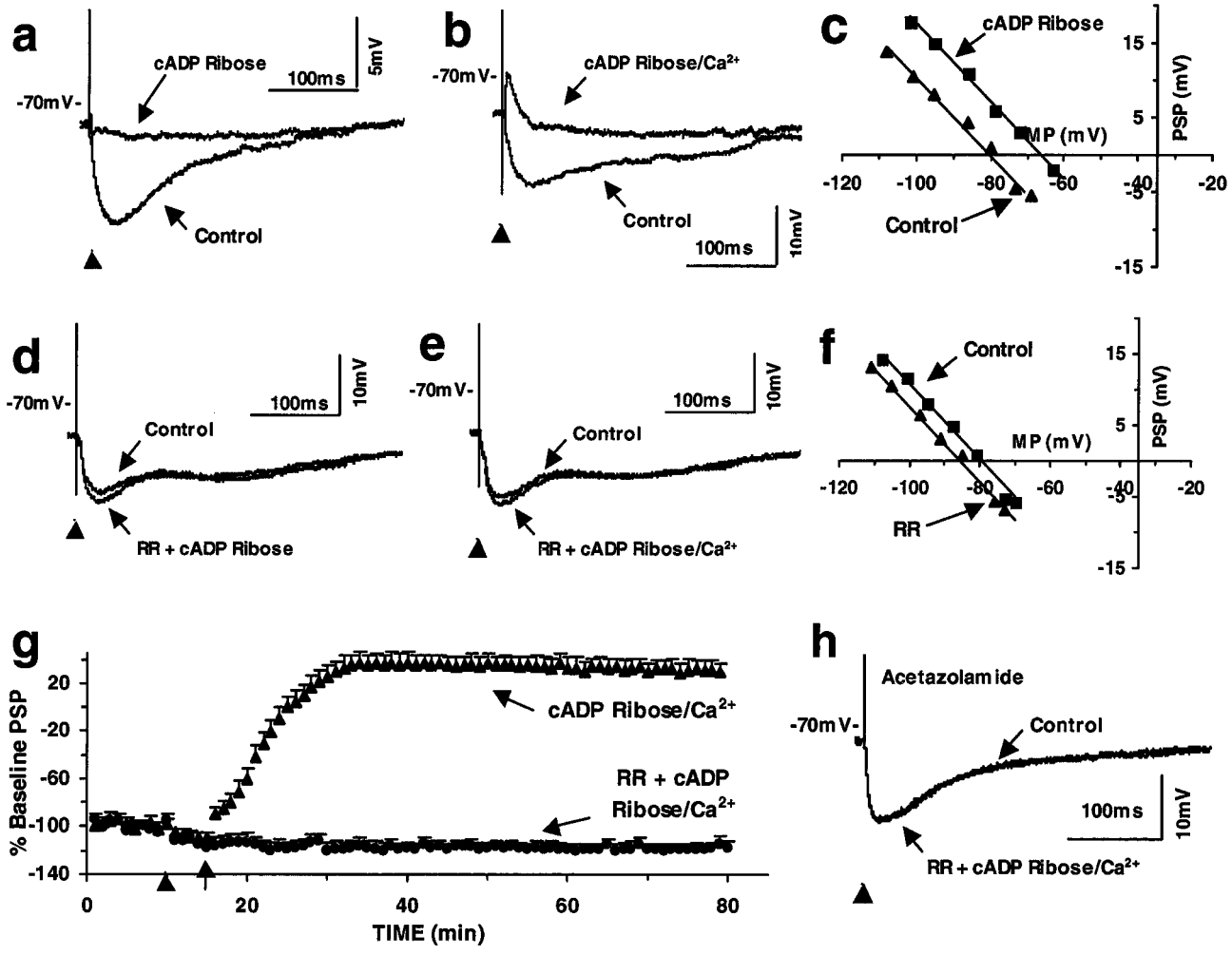

Fig. 3. (*a–c*) cADP-ribose reduces BAS-CA1 IPSP and reverses the IPSP to EPSP when associated with postsynaptic depolarization and shifts the potential response–membrane potential curve to the right. (*d–f*) RR prevents cADP-ribose- and cADP-ribose postsynaptic depolarization-induced changes in the BAS-CA1 responses and shifts the potential response–membrane potential curve to the left. (*g*) Time courses of the response to cADP-ribose postsynaptic depolarization (cADP-ribose/Ca^{2+}; at arrow) as compared with those of pre-RR application (at arrowhead); each point represents the mean PSP magnitudes + SEM normalized to the average of their control values before application of agents. In the cADP-ribose/Ca^{2+} group, the same procedure (sham injection of RR at arrowhead) also was applied through the electrode containing no RR. (*h*) Acetazolamide (1 μM, 30 min) prevents cADP-ribose postsynaptic depolarization-induced changes in the BAS-CA1 responses (40 min after cADP-ribose postsynaptic depolarization vs. control trace).

spatiotemporal patterning of cytosolic Ca^{2+} signals, including Ca^{2+} waves (4, 24), and in switching responses to low-frequency stimulation from long-term depression to long-term synaptic potentiation (25). Consistent with such a hypothesis are the observations that intracellular Ca^{2+} mobilization is altered in fibroblasts from patients with Alzheimer's disease (26) and that ischemia/stroke reduces RyR binding in the hippocampal CA1 (27). Decreases in calexcitin have been found in fibroblasts from the patients and can be induced by β-amyloid (28). Clarifying the underlying molecular mechanisms of RyR synaptic transformation may help elucidate pathophysiological involvement as well as cellular and molecular signal pathways important for higher cognitive processes.

RyR enables the endoplasmic reticulum to play an amplifying role in $[Ca^{2+}]_i$ elevation in neurons (29). It mobilizes Ca^{2+} from internal stores as a function of $[Ca^{2+}]_i$ (30, 31) by activating at least one isoform RyR_2 (32–34). cADP-ribose has been proposed to be a putative messenger (33, 35) of type 2 and type 3, but not type 1, RyRs. It releases Ca^{2+} from an inositol trisphosphate-insensitive mechanism in many mammalian cells (33, 36), including neurons (37–39). It increases the frequency of RyR Ca^{2+} channel opening in a planar lipid bilayer-incorporated preparation (33). The cADP-ribose concentration for half-maximal stimulation of Ca^{2+} from brain microsomes was reported (33) to be 100 nM (at extravesicular free Ca^{2+} concentration of 10^{-7} M). Others, however, reported that cADP-ribose concentrations higher than physiological range are needed to activate the RyR–channel complex (ref. 40; see ref. 22 for reviews). The requirement of higher concentrations may be due to the relatively lower amounts of luminal Ca^{2+} (40). In the present study, cADP-ribose is used as a pharmacological ligand. When diffused or injected into the recorded cells postsynaptically, it increased $[Ca^{2+}]_i$, reduced GABAergic inhibition by itself, and reversed the GABAergic postsynaptic responses when associated with postsynaptic depolarization. These results are consistent with the notion that the sensitivity of the RyR itself is regulated by $[Ca^{2+}]_i$. Nevertheless, the sensitivity of the responses to postsynaptic injection of RR indicates the essential role of RyR in the evoked responses.

The cADP-ribose depolarization-induced reversal of the GABAergic postsynaptic responses was sensitive to carbonic

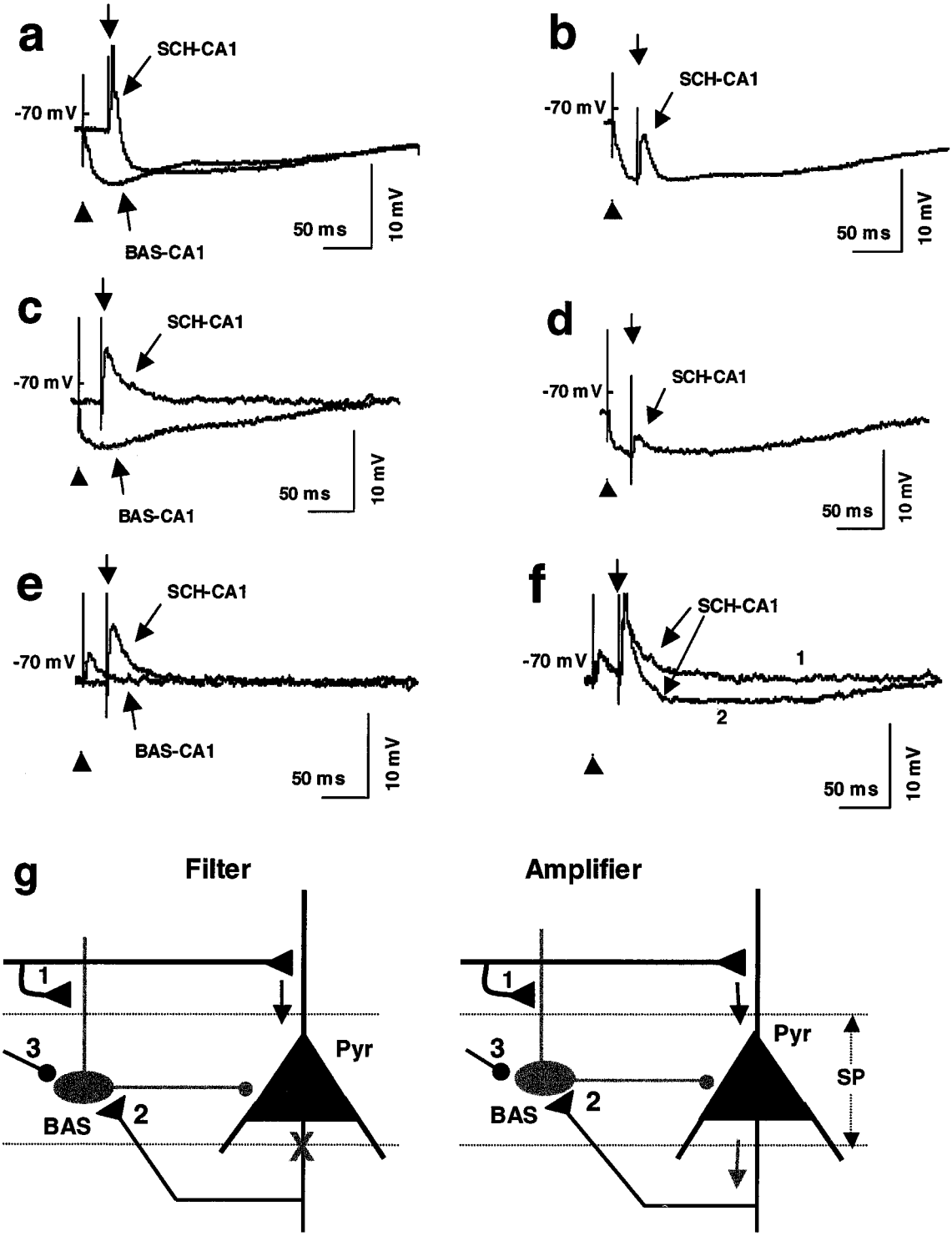

Fig. 4. Switching functions of GABAergic synapses from excitation filter to amplifier by RyR activation. (*a* and *b*) Single-pulse stimulation of BAS-CA1 (at arrowhead) and SCH [at above-threshold intensities; truncated; stimulated at arrow (*a*)] evokes an IPSP and action potentials, respectively. The excitatory SCH (at the same above-threshold stimulation) input is filtered out by a costimulation of BAS-CA1 (*b*). (*c–f*) Single-pulse stimulation (*c*) of BAS-CA1 and of SCH at below-threshold intensities evokes an IPSP and an EPSP, respectively. The excitatory SCH (at the same below-threshold stimulation) input is below threshold as evoked by costimulation (single pulse) of BAS-CA1 and SCH inputs (*d*) before cADP-ribose application. cADP-ribose (30 min after the application) transforms BAS-CA1 IPSP and does not change much of the SCH-CA1 EPSP, evoked by single-pulse stimulation of BAS or SCH, respectively (*e*). The excitatory SCH (at the same below-threshold stimulation) input is amplified by the co-BAS stimulation after the cADP-ribose-induced synaptic transformation and induces action potentials (truncated; *f*). Traces were from the same cell. (*g*) Schematic diagram of GABAergic inputs functioning as either excitatory filter (*Left*) or amplifier (*Right*). Active GABAergic inputs, either through activation of SCH as feed-forward inputs (no. 1), feedback inputs (no. 2), or of other circuits (no. 3; such as from the septum), effectively filter excitatory signals so that only very strong excitatory inputs might evoke action potentials. The GABAergic synaptic transformation results in amplifying excitatory signals so that weaker inputs can pass through the neural circuits. BAS, basket GABAergic interneurons (in gray); Pyr, CA1 pyramidal cells; SP, stratum pyramidale.

anhydrase inhibition. Carbonic anhydrase exists in CA1 pyramidal cells (41). The cellular mechanism underlying the RyR activation-induced GABAergic synaptic transformation thus apparently involves an induction of a depolarizing HCO_3^- flow through the GABA type A receptor–Cl^- channel. The HCO_3^- reversal potential is about −12 mV (42), so that an outward flux would result, depolarizing the membrane at the resting membrane potentials of neurons. Ca^{2+} may induce changes in anion selectivity of the Cl^- channels, activity of carbonic anhydrase, and/or formation of HCO_3^-, consistent with others' reports of reversing GABAergic inhibitory responses to depolarizing responses in neonates (43) that were caused by prolonged activation of GABA type A receptors (44) or the use of steroids (45).

The RyR activation-evoked reversal of the GABAergic postsynaptic responses may redirect signal transfer through the hippocampal network. Input signals that are strong enough to elicit action potentials in the pyramidal cells are filtered out by GABAergic inhibition. After the synaptic reversal, however, weak signals that are below action potential threshold are able to evoke action potentials when associated with the GABAergic inputs. It is important to mention that the synaptic reversal described here was produced postsynaptically. Thus, a widespread neuroexcitability would not be expected, even though one GABAergic BAS is known to innervate some 1,000 pyramidal cells. This type of synaptic plasticity can shape the intercommunication of hippocampal cells and, if produced *in vivo*, is likely to dramatically alter the signal processing in the hippocampus. Spatial learning increases the expression of RyR_2 in the rat hippocampus (46, 47). An enhancement of intracellular Ca^{2+} mobilization might be beneficial in terms of learning and memory or neurotoxic beyond a "health" range. It remains to be determined whether abnormality in the Ca^{2+} mobilization and synaptic plasticity may have pathologic consequence(s) such as memory impairment and, thus, might serve as therapeutic target(s).

1. Kornhauser, J. M. & Greeberg, M. E. (1997) *Neuron* **18,** 839–842.
2. Kleim, J. A., Vij, K., Ballard, D. H. & Greenough, W. T. (1997) *J. Neurosci.* **17,** 717–721.
3. Csicsvari, J., Hirase, H., Czurko, A. & Buzsaki, G. (1998) *Neuron* **21,** 179–189.
4. Berridge, M. J. (1998) *Neuron* **21,** 13–26.
5. Berridge, M. J., Bootman, M. D. & Lipp, P. (1998) *Nature (London)* **395,** 645–648.
6. Alkon, D. L., Nelson, T. J., Zhao, W. Q. & Cavallaro, S. (1998) *Trends Neurosci.* **21,** 529–537.
7. Hardingham, G. E., Cahwla, S., Johnson, C. M. & Bading, H. (1997) *Nature (London)* **385,** 260–265.
8. Golovina, V. A. & Blaustein, M. P. (1997) *Science* **275,** 1643–1648.
9. Korkotian, E. & Segal, M. (1998) *Eur. J. Neurosci.* **10,** 2076–2084.
10. Sun, M.-K. & Reis, D. J. (1994) *J. Physiol. (London)* **476,** 101–116.
11. Collin, C., Devane, W. A., Dahl, D., Lee, C.-J., Axelord, J. & Alkon, D. L. (1995) *Proc. Natl. Acad. Sci. USA* **92,** 10167–10171.
12. Stuart, G. J., Dodt, H. U. & Sakmann, B. (1993) *Pflügers Arch.* **423,** 511–518.
13. Grynkiewicz, G., Poenie, M. & Tsien, R. Y. (1985) *J. Biol. Chem.* **260,** 3440–3450.
14. Sun, M.-K., Nelson, T. J., Xu, H. & Alkon, D. L. (1999) *Proc. Natl. Acad. Sci. USA* **96,** 7023–7028.
15. Collingridge, G. L. & Lester, A. J. (1989) *Pharmacol. Rev.* **40,** 143–209.
16. Buhl, E. H., Halasy, K. & Somogyi, P. (1994) *Nature (London)* **368,** 823–828.
17. Cobb, S. R., Buhl, E. H., Halasy, K., Paulsen, O. & Somogyi, P. (1995) *Nature (London)* **378,** 75–78.
18. Cobb, S. R., Halasy, K., Vida, I., Nyiri, G., Tamas, G., Buhl, E. H. & Somogyi, P. (1997) *Neuroscience* **79,** 629–648.
19. McMahon, L. L. & Kauer, J. A. (1997) *Neuron* **18,** 295–305.
20. Paulsen, O. & Moser, E. I. (1998) *Trends Neurosci.* **21,** 273–278.
21. Sharp, A. H., McPherson, P. S., Dawson, T. M., Aoki, C., Campbell, K. P. & Snyder, S. H. (1993) *J. Neurosci.* **13,** 3051–3063.
22. Zucchi, R. & Ronca-Testoni, S. (1997) *Pharmacol. Rev.* **49,** 1–51.
23. Xu, L., Eu, J. P., Meissner, G. & Stamler, J. S. (1998) *Science* **279,** 234–237.
24. Ding, J. M., Buchanan, G. F., Tischkau, S. A., Chen, D., Kuriashkina, L., Faiman, L. E., Alster, J. M., McPherson, P. S., Campbell, K. P. & Gillette, M. U. (1998) *Nature (London)* **394,** 381–384.
25. Wang, Y., Wu, J., Rowan, M. J. & Anwyl, R. (1996) *J. Physiol. (London)* **495,** 755–767.
26. Ito, E., Oka, K., Etcheberrigaray, R., Nelson, T. J., McPhie, D. L., Tofel-Grehl, B., Gibson, G. E. & Alkon, D. L. (1994) *Proc. Natl. Acad. Sci. USA* **91,** 534–538.
27. Nozaki, H., Tanaka, K., Gomi, S., Mihara, B., Nogawa, S., Nagata, E., Kondo, T. & Fukuuchi, Y. (1996) *Neurochem. Res.* **21,** 975–982.
28. Kim, C. S., Han, Y. F., Etcheberrigaray, R., Nelson, T. J., Olds, J. L., Yoshioka, T. & Alkon, D. L. (1995) *Proc. Natl. Acad. Sci. USA* **92,** 3060–3064.
29. Chavis, P., Fagni, L., Lansman, J. B. & Bockaert, J. (1996) *Nature (London)* **382,** 719–722.
30. Clapper, D. L., Walseth, T. F., Dargie, P. J. & Lee, H. C. (1987) *J. Biol. Chem.* **262,** 9651–9658.
31. Lee, H. C., Walseth, T. F., Bratt, G. T., Hayes, R. N. & Clapper, D. L. (1989) *J. Biol. Chem.* **264,** 1608–1615.
32. Galione, H. C., Lee, H. C. & Busa, W. B. (1991) *Science* **253,** 1143–1146.
33. Mészáros, L. G., Bak, J. & Chu, A. (1993) *Nature (London)* **364,** 76–79.
34. Sitsapesan, R., McGarry, S. J. & Williams, A. J. (1994) *Circ. Res.* **75,** 596–600.
35. Lee, H. C. (1997) *Physiol. Rev.* **77,** 1133–1164.
36. Takasawa, S., Nata, K., Yonekura, H. & Okamoto, H. (1993) *Science* **259,** 370–373.
37. Currie, K. P., Swann, K., Galione, A. & Scott, R. H. (1992) *Mol. Biol. Cell.* **3,** 1415–1425.
38. Hua, S. Y., Tokimasa, T., Takasawa, S., Furuya, Y., Nohmi, M., Okamoto, H. & Kuba, K. (1994) *Neuron* **12,** 1073–1079.
39. Linde, D. J., Dawson, T. M. & Dawson, V. L. (1995) *J. Neurosci.* **15,** 5098–5105.
40. Sitstapesan, R., McGarry, S. J. & Williams, A. J. (1995) *Trends Pharmacol. Sci.* **16,** 386–391.
41. Pasternack, M., Voipio, J. & Kaila, K. (1993) *Acta Physiol. Scand.* **148,** 229–231.
42. Staley, K. J., Soldo, B. L. & Proctor, W. R. (1995) *Science* **269,** 977–981.
43. Leinekegel, X., Khalinov, I., McLean, H., Caillard, O., Gaiarsa, J. L., Ben-Ari, Y. & Khazipov, R. (1999) *Adv. Neurol.* **79,** 189–201.
44. Staley, K. J. & Proctor, W. R. (1999) *J. Physiol. (London)* **519,** 693–712.
45. Burg, M., Heinemann, U. & Schmitz, D. (1998) *Eur. J. Neurosci.* **10,** 2880–2886.
46. Cavallaro, S., Meiri, N., Yi, C. L., Musco, S., Ma, W., Goldberg, J. & Alkon, D. L. (1997) *Proc. Natl. Acad. Sci. USA* **94,** 9669–9673.
47. Zhao, W., Meiri, N., Xu, H., Cavallaro, S., Quattrone, A., Zhang, L. & Alkon, D. L. (2000) *FASEB J.* **14,** 290–300.